Chapter 4

Eichhorniacrassipes (Jalkumbhi) bio-waste derived Activated Carbon: Study of morphology and their electro-chemical activity for supercapacitor application

This chapter deals with the general discussion about porosity in material for enhanced performance. After that, it also describes the synthesis of high porous electro-active carbon materials from bio-waste via pyrolysis methods using the N_2 atmosphere and well characterized. This porous electro-active carbon is used as electrode material for supercapacitor application.

4.1. Introduction

The electrochemical supercapacitor is an energy storage device that has been considered reasonable means throughout worldwide to solve the energy crisis due to their unique performance as high-power density, fast charge-discharge rate, and excellent reversibility [Liu et al. (2016), Gou et al. (2020), Simon et al. (2008)]. A series of metal oxides, traditional carbon nanomaterials, conducting polymers, metal-organic frameworks (MOFs) are reported for supercapacitor applications with the functional mechanism as non-faradic charge storage at the electrode-electrolyte interface called electrolytic double-layer capacitor (EDLC) and via faradic or redox process (pseudo-capacitor) [Azad et al. (2018), Gupta et al. (2009), uzaffar et al. (2019)]. Due to chemical precursors and complicated preparation procedures, which are expensive and environmentally harmful, such materials are less suitable/compatible in the field of renewable energy devices and supercapacitors. While natural organic materials (plants and animals) have rich carbon content and with some heteroatoms, so the bio-wastes are now considered as an eco-friendly source for sustainable carbon nanomaterials. The special hierarchical structures, abundant surface area, as well as electrical properties of biowaste derived activated carbons, gives a significant status and are getting more attention to the electrochemical application. Thus, at present, the biomass-waste derived AC has been nominated as sustainable electrode materials with compatible electrochemical reaction processes such as ion transfer and diffusion. Therefore, the preparation of activated carbon by natural biowastes has become a hot topic in the field of energy storage and conversion. The American Water Works Association (AWWA) B600 announced a standard specific surface area (SSA) in a range of 500 $m^2 g^{-1}$ or more for

the ACs [Xia et al. (2016)]. In earlier works, it has been quoted that the ACs prepared from bio-wastes are a sweltering field [Hirst et al. (2018), Tamilselvi et al. (2020)]. Since a large number of biomass wastes formed not only throughout the country but globally also, they may cause contamination and dirty environment. Therefore, contamination management and recycling technology are paying great attention in the present time to protect the environment and consequently generating new activated and highly porous carbon nanomaterials which can be used for various applications such as gas separation and storage, hydrogen storage, energy storage systems, toxic heavy metal detection, semiconductors, electrocatalysis and so on [Hirst et al. (2018), Zhang et al. (2018), Biswal et al. (2013), Pinero et al. (2009), Madhu et al. (2014), Zhu et al. (2018), Reddy et al. (2013), Xia et al. (2016)]. Various reports are published to derived AC from waste as in Table 1.1.

Carbonization or pyrolysis is a very simple process for the production of activated carbon (AC) and has been reported for a long time. The carbon formed by the pyrolysis method is usually required some chemical activation (using such chemicals like KOH, NaOH, H_3PO_3 etc), and sometimes the resulted carbon is self-activated. The biomass gases (CO_2, NH_3, and CH_4, H_2O) produced during pyrolysis can serve as self-activating agents to give activated carbon [Mohan et al. (2006)]. Therefore, the selection of the source, subjected to pyrolysis, is also an essential step for the production of AC. *Eichhorniacrassipes* locally known as Jalkumbhi is spongy biomass consisting of a huge number of air bladders and moisture. Obviously, due to gases and moisture, this plant can provide a new resource for self-activated high value-added carbon materials. India is one of the world's leading countries having

diverse cultivation in the aquatic phase, e.g. river, ponds and lakes, producing a good percentage of the economy of the country. *Eichhorniacrassipes* found throughout India, is an aquatic plant, floating on lakes and water ponds, a bio-waste and also known as a terror of Bengal [Asmare et al. (2017)]. Therefore, cleaning and transformation of such unwanted herbs are necessary to protect aquatic life. Due to the high percentage of water content and porous nature, the *Eichhorniacrassipes* may produce activated carbon with high surface area and porous structure, which is a primary requirement for supercapacitor electrode materials. Keeping all these points in mind, we proposed the preparation of ACs from the *Eichhorniacrassipes* plant. We aim to demonstrate a general route for the development of AC from the biomass wastes of *Eichhorniacrassipes* via carbonization under an inert atmosphere. For the more detailed inspection, three different kinds of ACs synthesized by variation of carbonization temperatures (600, 700 and 800ºC). Further, structural identification of such material was carried out using various techniques like XRD, FTIR, Raman and FE-SEM. TGA has been used to check thermal sustainability, and BET has performed to understand its porous nature and active surface area. Furthermore, the electrochemical performances of the as-synthesized nanohybrids have been conducted for realize their supercapacitive behavior using Nafion as a binder and activated acetylene black as a conductive component. A good agreement has been observed between morphological characterization and electrochemical performance.

4.2 Materials and methods

4.2.1 Materials

Jalkumbhi was received from a pond of Seer Govardhan village nearby Banaras Hindu University, Varanasi. Potassium bromide (KBr), sulphuric acid (H_2SO_4), and hydrogen fluoride (HF) purchased from Merck, India used as received. Double distilled water (DDW) water collected from CIF IIT (BHU).

4.2.2Synthesis of ECCs

ECC was prepared by the carbonization process under inert conditions (N_2 atmosphere) without any chemical activation [Madhu et al. (2014)]. Herein this process, *Eichhorniacrassipes* (Jalkumbhi) leaves were collected in large quantity from the source, washed with tap water for several times and twice with ultrapure water subsequently followed by ethanol to remove mud. Finally, this washed *Eichhorniacrassipes* was put in the hot-air oven at 80ºC for 24 hours to remove water content and crushed using mortar pestle to get a fine powder. The obtained powder was loaded in an alumina boat and transferred in the tubular furnace for carbonization at the three desired temperatures (600, 700 and 800ºC) for 3h under an inert atmosphere with heating rate 10ºC min^{-1} which was followed by natural cooling to room temperature. The ACs were washed carefully using 1.0 M HCl and 1.0 M HF to remove inorganic contaminants, washed several times with ultrapure water, and dried in a vacuum oven at 80ºC for 24 hours. After that, this ACS was ground to make a fine powder and used for further characterizations. A schematic representation of the synthesis process of ECC is presented in Figure 4.1.

Figure 4.1 Schematic representation for the synthesis of ECCs.

4.2.3 Modification of Working Electrode

Polished GC electrode was modified with a calculated amount of as-prepared ink having as-synthesized materials, acetylene black and Nafion. Prior to every modification, the GC electrode was appropriately polished using 0.03 μM alumina slurry on a polishing pad. After that, homogeneous ink was prepared by mixing 80% active materials,10% acetylene black and 10% Nafion (Nafion of 5 wt % in water) by mass in ethanol followed by sonication for 30 minutes. Subsequently, 10 μL of this ink was drop casted on the GC surface and dried at room temperature.

4.3. Results and discussion

4.3.1 Structural analysis

XRD pattern:

To verify the successful formation AC, XRD were performed as depicted in Figure 4.2. Except for a few remarkable observations, all ECCs exhibit almost similar type of broad diffraction patterns due to its amorphous background. The XRD spectra of all ECCs showing one broad characteristic peaks at 2θ=25° corresponding to (002) plane. Another

diffraction peak at 2θ=43.6° is observing at an elevated temperature only due to (100) plane of graphitic carbon, indicating the higher % of graphitic carbon in the case of ECC 800 [Zhang et al. (2018), Biswal et al. (2013) , Shang et al. (2015) , Subramaniyam et al. (2017) , Wang et al. (2018)].

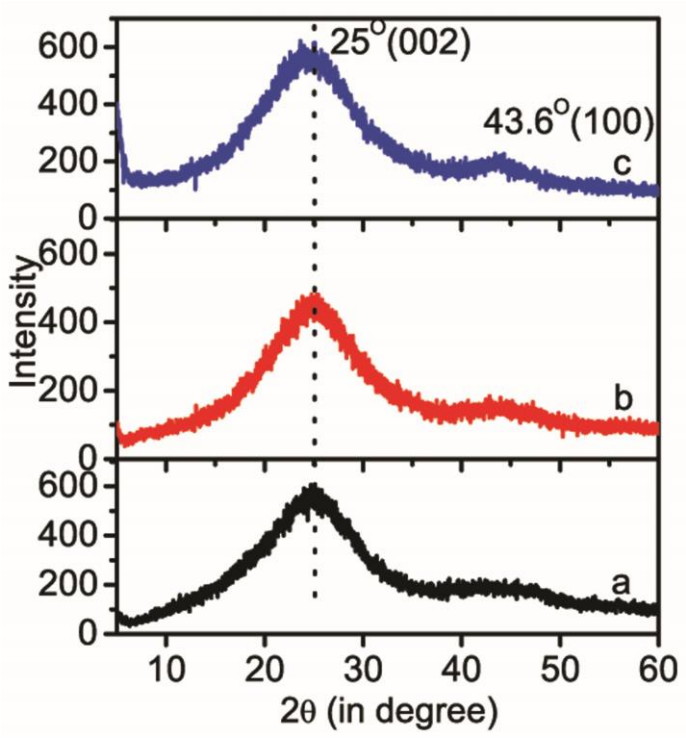

Figure 4.2: XRD analysis of the as-prepared ACs prepared at different temperatures (a) ECC 600, (b) ECC 700 and (c) ECC 800.

FT-IR analysis:

To check the structural and functional groups of synthesized materials, the FT-IR spectra of ACs were recorded by the KBr pellet technique (Figure 4.3I). The close resemblance between FT-IR spectral profiles indicates the presence of similar functional group in all samples. All ACs samples exhibit a band at 3419 cm^{-1} corresponding to –OH hydroxyl groups. The sharp band around 1567 cm^{-1} attributed to C=C stretching vibrations or aromatic ring which clarifies that such material has an

sp^2 hybridized π-conjugated system. A broadband in range ~1010–1100 cm^{-1}, which indicates the presence of the C–O bond of alcohols, carboxylic acids, phenols and esters [Inala et al. (2018)]. Raman spectroscopy was used to confirm the disorderness of graphitic domains in ECC 800. Two characteristics peaks centered at 1316 cm^{-1} and 1600 cm^{-1} due to so called D-and G-band associated with disordered carbon and in-plane vibration of graphitic domain respectively (*see* Figure 4.3II) [Biswal et al. (2013), Wahid et al. (2014)]. Such carbon materials does not show 2D band in raman because of highly doped heteroatom level and lack of layered and well aligned structure. The 2D band shape of raman is consiqunce of few layer of graphene.

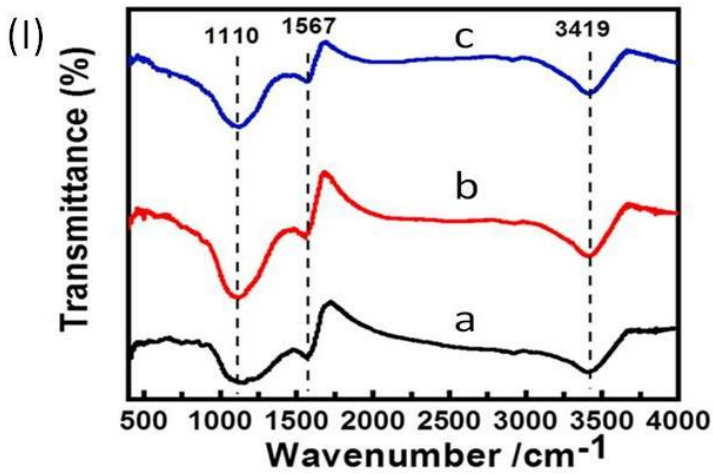

Figure 4.3I FT-IR analysis of the as-prepared ACs prepared at different temperatures (a) ECC 600, (b) ECC 700 and (c) ECC 800.

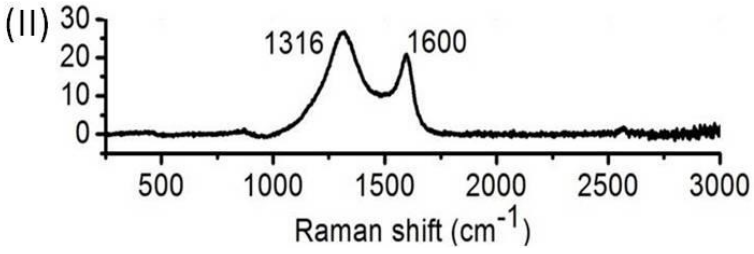

Figure 4.3II Raman spectra of ECC 800.

4.3.2 Morphology and microstructure analysis:

To assess the morphology and microstructure of the prepared ACs samples, SEM imaging has been performed (Figure 4.4). This SEM image discloses their morphological textures which are directly related to the carbonization temperature. As shown in Figure 4.4c, ECC 800 has more open porous sites and a network of hollow chambers compared to ECC 600 and ECC 700 (Figure 4.4a and 4.4b). At lower temperatures, the material texture found in the agglomerated state because of the presence of some parental functional groups. However, these chemicals may eliminated when the high temperature is applied during pyrolysis [Mohan et al. (2006)].

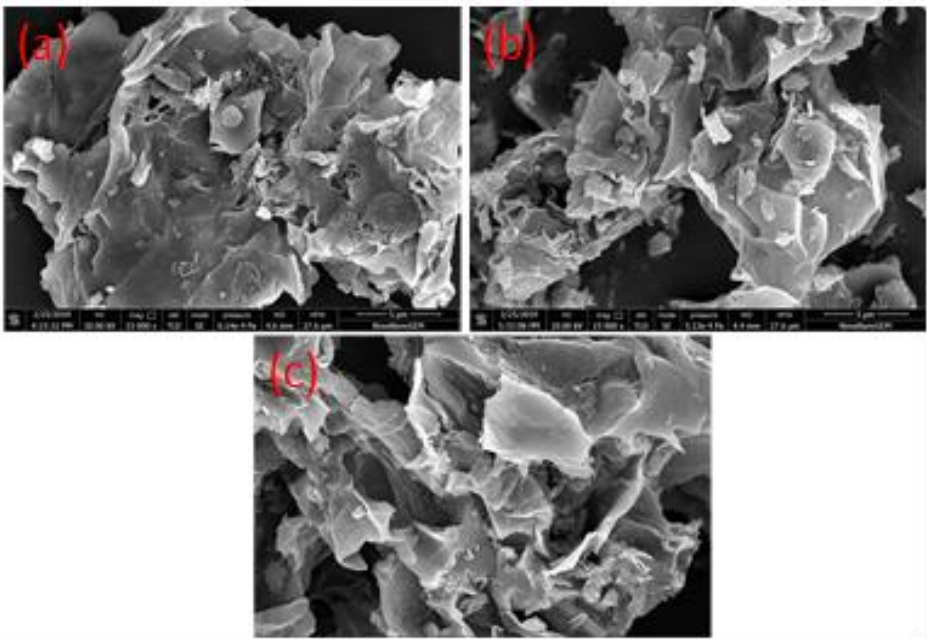

Figure 4.4 SEM image of (a) ECC 600, (b) ECC 700, (c) ECC 800.

Therefore, among these three samples, ECC 800 showed a high degree of surface roughness and the porous structure, is prone to provide a good capacitive performance (shown in electrochemical analysis part), because of the hierarchical morphology with

a high surface area which provides fast diffusion of electrolyte-charges along pore channels [Jung et al. (2018)].

4.3.3 BET surface area analysis:

To find out the actual surface area and the porosity of synthesized materials, N_2 adsorption-desorption analysis was performed (as depicted in Figure 4.5). According to 'International Union of Pure and Applied Chemistry (IUPAC)' proposal, the samples ECC 600 and ECC 700 have Type-IV adsorption isotherm with open loops having less surface area and porosity (Figure 4.5a-b). The hysteresis loops are not close in the case of ECC 600 and ECC 700 samples even under very low pressure. This can be due to numerous reasons. First, structural deform induced by adsorption and trapped N_2 cannot be fully released because of the heterogeneous surface. N_2 uptake capacity increases with an increase in the carbonization temperature from 600 to 800°C indicating the gradual formation of the porous structure. ECC 800 adsorption-desorption isotherms as presented in Figure 4.5c, accompanying the Type IV with H_4 hysteresis loop, which indicates the existence of a mixture of microporous and mesoporous structures [Madhu et al. (2014), Kumar et al. (2016), Wahid et al. (2014)]. Further, the estimated pore size and pore volume of these samples are summarized in Table 4.1. The average pore diameter decreases and pore volume increases from ECC 600 to ECC 800. This result reveals that when the temperature increases from 600 to 800°C during carbonization, the BET surface area increased drastically from 109, 308 to 780 m^2g^{-1} for ECC 600, ECC 700 and ECC 800, respectively.

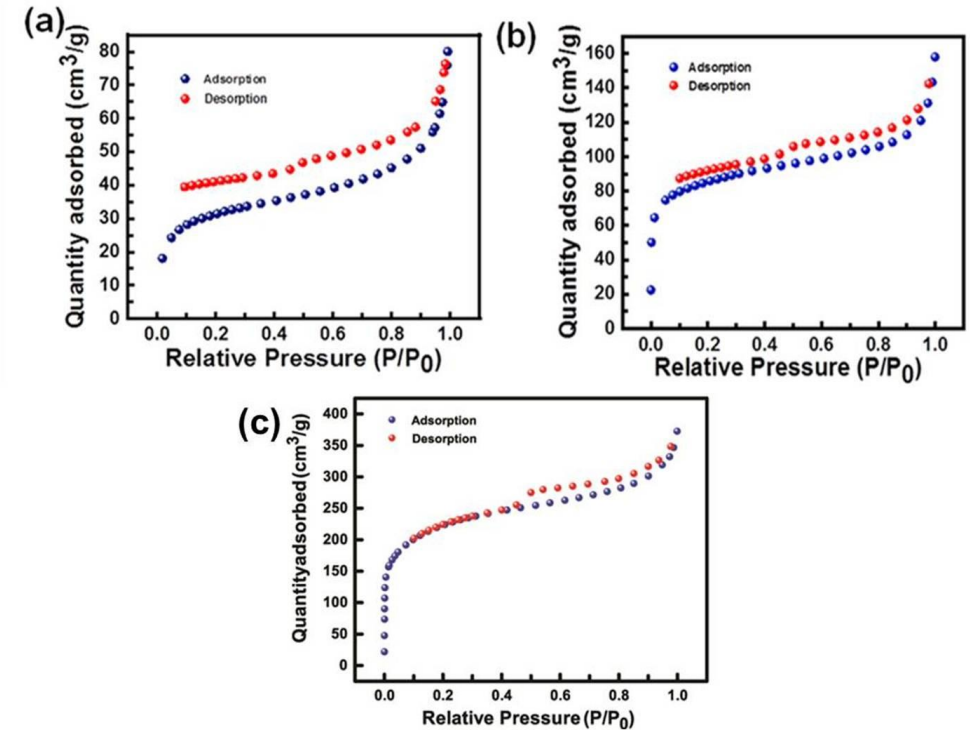

Figure 4.5 N_2 adsorption-desorption isotherms of (a) ECC 600, (b) ECC 700, (c) ECC 800.

This trend indicates that the primary micropores are produced mainly by the loss of water content under lower temperatures, but at high-temperature various gases and other constituents were eliminated in the form of gas leading to high surface area mesoporous graphitic carbon. Since the meso-/micro-pores may offer transportation and diffusion channels for electrolyte-ion, and the micropores recommend the space for ion storage [Bi et al. (2019)]. Hence, ECC 800 may exhibit better capacitance than ECC 600 and ECC 700.

Table 4.1. BET surface area and other parameters for ECC 600, ECC 700, and ECC 800.

Sample	BET surface area (10^2 m^2g^{-1})	Pore volume(cm^3g^{-1})	Pore diameter(nm)
ECC 600	1.096	0.1222	4.4582
ECC 700	3.089	0.2235	2.8937
ECC 800	7.807	0.5465	2.8003

4.3.4 Thermogravimetric analysis:

The pyrolysis temperature of *Eichhorniacrassipes* was optimized by TGA (see inset of Figure 4.6). It can be seen that dried *Eichhorniacrassipes* exhibit gradual mass loss since the application of temperature and shows a sudden loss in the range 221- 460^{o}C due to the removal of moistures followed by decomposition of organic components [Haffner-Staton et al. (2016)]. After that, the curve is exhibiting a very slight slope and tending to parallel with the temperature-axis. This is due to the slow decomposition of carbon in the biochar. After 850^{o}C, this stage material exhibits further decomposition of carbon components. Thus in this way, we have chosen 600^{o}C, 700^{o}C and 800^{o}C to pyrolyze *Eichhorniacrassipes*. On pyrolysis, all ECC exhibits first moisture removal at 100^{o}C and another single and sharp stage of burn-off degradation (450^{o}C for ECC 600, 503^{o}C for ECC 700 and 522^{o}C for ECC 800). It means that carbonaceous matters are uniform in nature. However, the shifting of the curve towards a higher temperature side probably due to a higher extent of graphitic domains on increasing the pyrolysis temperature from 600^{o}C to 800^{o}C (*cf.* Figure 4.6a, Figure 4.6b and Figure 4.6c). That is why we are observing slight crystallinity in XRD (appearance of (100) plane at 43.6^o; (*cf*. Figure 4.2) at the higher temperature.

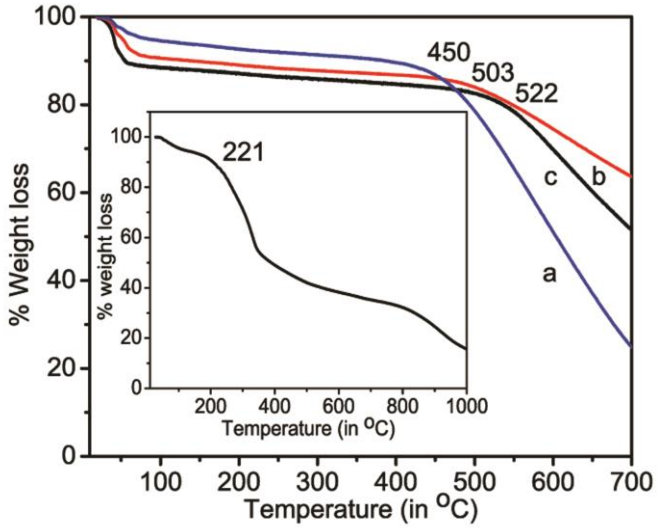

Figure 4.6: TGA of (I) (a) ECC 600, (b) ECC 700, (c) ECC 800,. Inset shows TGA of (a) dried *Eichhorniacrassipes.*

4. 3.5 Electrochemical measurement

The electrochemical performances of as-prepared ECCs were investigated by electrochemical methods (e.g. CV, GCD and EIS techniques). First of all, CV were performed for all ECCs in 1.0 M H_2SO_4 electrolyte solution with the variation of scan rates at the non-Faradic potentiodynamic condition from 0 to 1.0 V (Figure 4.7). From these results, it is evident that the CV curves of all ECCs are almost rectangular shape, revealing that these materials followed the electric double-layer capacitance (EDLC) mechanism to store the charges/ions [Inala et al. (2918), Zhang wt al.(2018), Wahid et al. (2014)]. At the same time, the CV area under the curves is directly proportional to scan rate in all the cases and CV curve shape was maintained throughout scan rates variation from 20, 70 100 and 150 mV/s. This observation is implying a facile and quick dynamics movement (adsorption and desorption) of the electrolyte ions onto the working electrode (Figure 4.7I, Figure 4.7II and Figure

4.7III) [Purkait et al. (2017), Razmjooei et al. (2017), Liang et al. (2014), Biswal et al. (2013)]. On comparing the CV curve of ECC 600, ECC 700 and ECC 800 at scan rate 150 mV/s, ECC 800 exhibits higher area under the curve than that of ECC 600 and ECC 700, suggesting higher charge storage among other [Wahid et al. (2014)] (as shown in Figure 4.7IV). This result can be emphasized that higher temperature pyrolysis of biomass, resulting in a graphitic structure with a highly porous and larger surface area, can increase the capacity to accelerate the charges/ions store [Tamilselvi et al. (2020), Purkait et al. (2017)]. Figure 4.7V is a Randles−Sevcik equation derived plot showing a liniear relation between current density and scan rate and it evident that electrochemical process is diffusion controlled process [piriya et al. (2018)].

To investigate the real capacitive properties, the GCD experiment has done using the same condition. Figure 4.8IVa-c shows comparative charge-discharge curve of all samples (ECC 600, ECC 700 and ECC 800) at current density 0.78 A/g. ECC 800 exhibits sufficiently long charge-discharge interval compared with ECC 600 and ECC 700, suggested that the ECC 800 has a superior potential for supercapacitor. Their charge-discharge profile at different current density 0.78, 1.31, 1.84, 2.36 and 2.89A/g. is represented as in Figure 4.8I-III. As can be seen, all GCD curves show typical symmetrical triangular shape revealing that as-synthesized material has a good reversibility nature for charge accumulation and coulomb efficiency, which are fundamental requirements for supercapacitor [Zhou et al. (2013)].

Further specific capacitance (Csp) vs current density of all electrode materials is calculated based on GCD curves using the following equation (1) and tabulated in table 4.2.

$$C_s = \frac{I * \Delta t}{m * \Delta V} \quad \text{.....(1)}$$

where C_s (F/g) is the specific capacitance, I (A) is the applied current, ΔV (V) is a potential window, and m (g) is mass of active electrode material loaded on the working electrode.

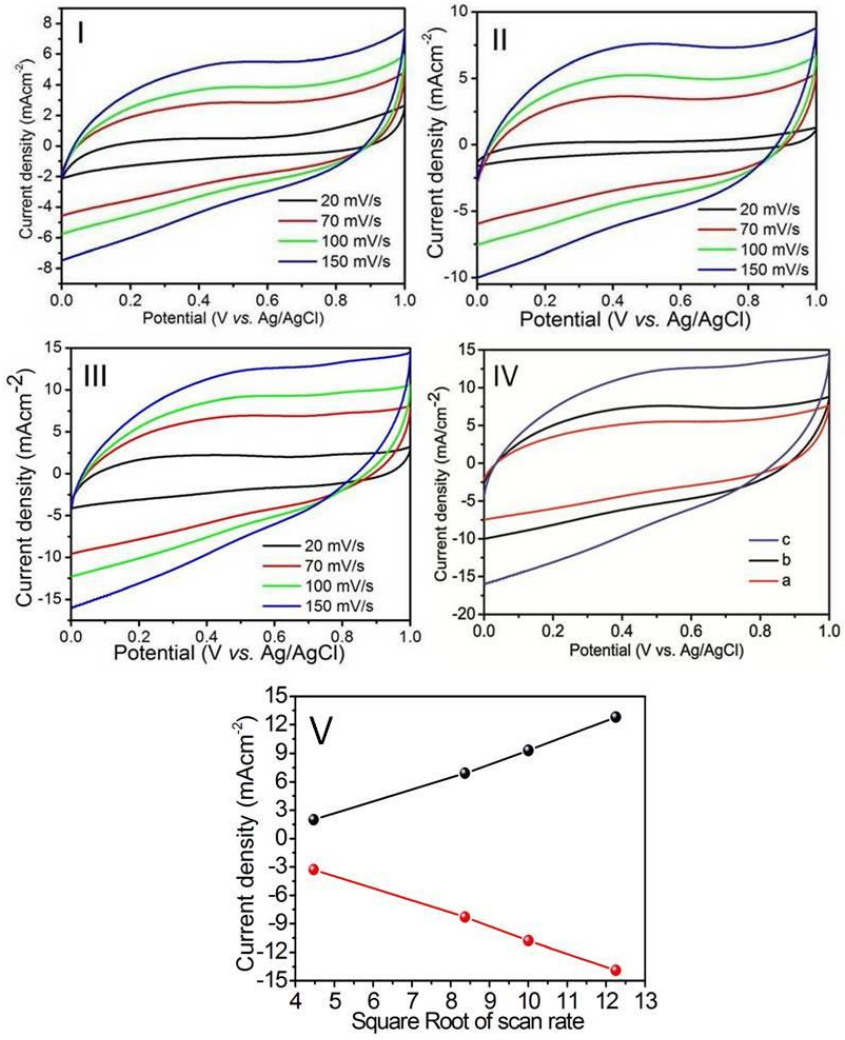

Figure 4.7CV of (I) ECC 600 (II) ECC 700, (III) ECC 800 at different scan rates in 1.0 M H_2SO_4 and (d) comparative CV of (a) ECC 600, (b) ECC 700, and (c) ECC 800 at 150 mV/s scan rate, and (VI) current density *vs.* square root of scan rate plot for ECC 800.

The GCD results showed the maximum specific capacitance of ECC 800 is 292.64 F/g at a current density of 0.78 A/g, which is comparably higher than those reported for biomass-derived porous carbons in table 4.3. This superior electrochemical performance of ECC 800 can be attributed to it having a porous structure with a large specific surface area which could provide more accessible channels for the movement of charge/ions [Wahid et al. (2014)]. The specific capacitance of ECC 800 (from Figure 4.8III and Table 4.2) varies from 292.64F/g at 0.78A/g to 237.62F/g at 2.89A/g.

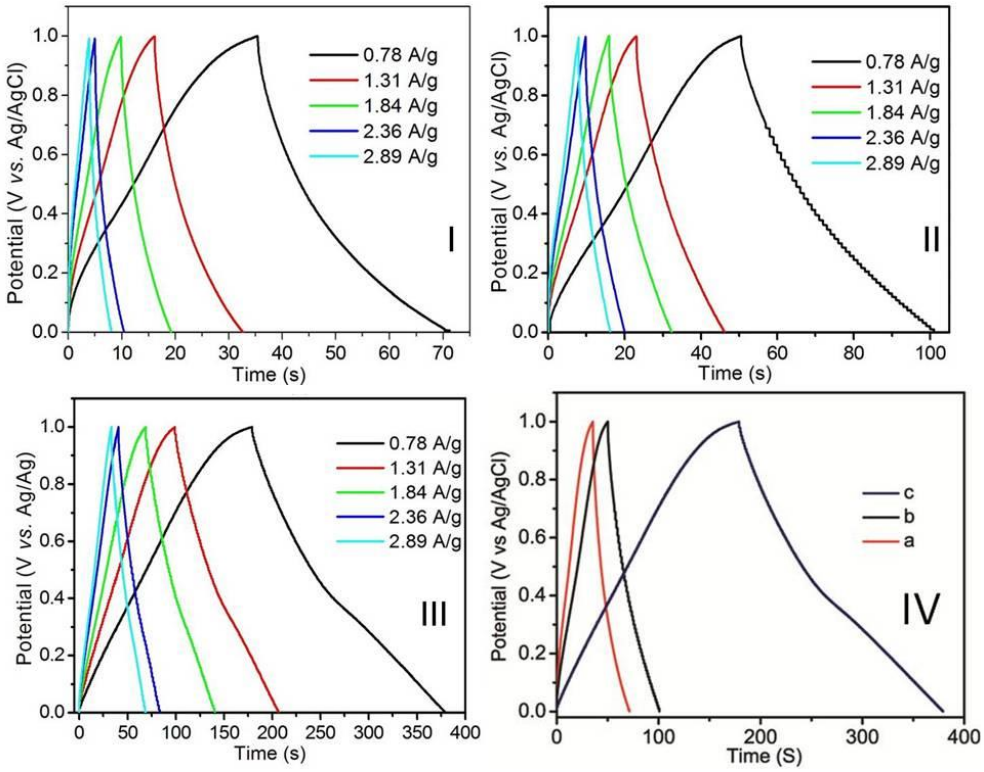

Figure 4.8 GCD profiles of (I) ECC 600, (II) ECC 700 and (III) ECC 800 at various current densities and (IV) comparative charge-discharge profiles of (a) ECC 600 (b) ECC 700, (c) and ECC 800 at current density=0.78A/g.

In order to examine the charge impedance between the modified working electrode and the reference electrode, EIS was performed for all ECC materials in the frequency

range from 100 kHz to 10.0 mHz as shown in Figure 4.9. The Nyquist plot gives a roadmap to evaluate internal resistance, charge transfer resistance and ion diffusion route. Usually, it has been interpreted that Nyquist plot consists of two regions: the first one is nearly at low frequency showing a vertical straight line, and another a semi-circle (on Z'-axis) like shape appeared at high frequency and inclination of the curve towards Z''-axis is the consequence of high charge accumulation on electrode surface [Subramanya et al. (2015), Kumar et al. (2011)]. From Nyquist plot, on comparing ECC 600, ECC 700 and ECC 800, ECC 800 is exhibiting more capacitive behavior because the vertical straight line is more inclined towards imaginary axis (Z"-axis) as well as the lowest value of Z" in the low-frequency region (*cf.* Figure 4.9 a-c). This results also supportive to our earliar resulst in CV and GCD and verifyed that the superior supercapacitive nature of ECC 800.

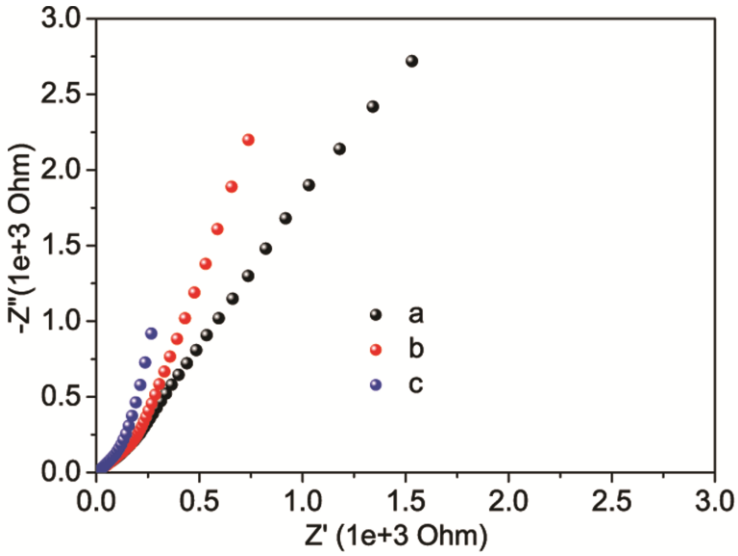

Figure 4.9 EIS of (a) ECC 600, (b) ECC 700 and (c) ECC 800

The durability and stability of the catalyst is a critical factor for their real and practical application. To access the durability and stability of the best ECC 800, we performed multiple cycles of CVs for 250 continuous cycles from 0 to 1.0 V at 50 mV/s in 1 M H_2SO_4 (Figure 4.10). It was found that no significant change in the current density, the CV curves traces the same path without any variation. This reveals the superior cycling stability of the catalyst towards capacitive application. The optimal electrodes exhibit good stability, at the initial stage the area under the CV curve become expand (2^{nd} to 50^{th} cycle in Figure 4.9) and after that, the CV curves trace the same path. This is because of swelling in the electrode materials under initial potential ramping and permitted more charge. After this, the electrode becomes equilibrium or saturated.

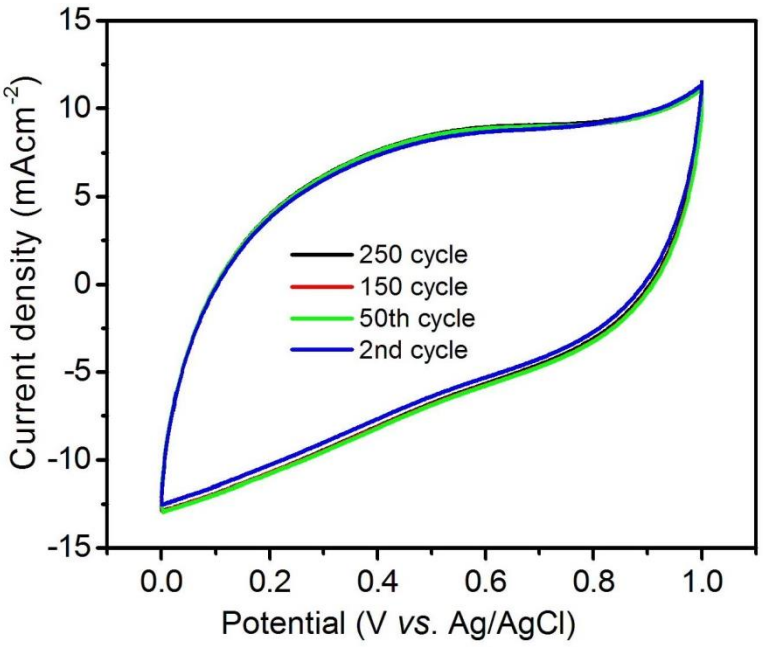

Figure 4.10 stability test of the ECC 800 *via* multiple CV at 50 mV/s scan rate.

Table 4.2. The specific capacitance of the ECC 600, ECC 700 and ECC 800 at different current densities.

Current density (A/g)	Specific capacitance (C_s) (F/g)		
	ECC 600	ECC 700	ECC 800
0.78	54.97	78.94	292.64
1.31	42.39	60.76	270.86
1.84	34.98	59.87	257.97
2.36	29.82	57.28	239.81
2.89	22.22	54.58	237.62

Table 4.3. Comparative capacitive profiles for activated carbons derived from various biomasses reported earlier.

	Capacitance value (F/g)	Electrolyte	Cell configurat-ion	Ref.
Ginkgo leaf derived carbon material	272.0	1 M H_2SO_4	2	Zhu et al. (2018)
Cassava peel waste	153.0	0.5 M H_2SO_4	3	Ismanto et al.(2010)
Urine carbon	254.12	6.0 M KOH	3	Razmjooei et al. (2017)
Cotton pulp sheet	107.0	5 M KCl	3	Jiang et al.(2016)
Waste coffee beans	100.0	1.0M $TEABF_4$/ ACN	3	Rufford et al.(2009)
Rice husks	147.0	6 M KOH	2	Teo et a. (2016)
Carbon Fiber	180.1	1M H_2SO_4	2	Ma et al. (2016)
Cumin plant waste	155.0	1M H_2SO_4	2	Inal et al. (2018)
Sugarcane bagasse	280.0	1MH_2SO_4	3	Wahid et al. (2014)
Dead Neem leaves	88.0	1 M H_2SO_4	2	Biswal et al. (2013)

4.4 Conclusions

In summary, the ACs derived from *Eichhorniacrassipes* was synthesized successfully, through high-temperature pyrolysis. The obtained ECC 800 ACs have a large specific surface area (780 m^2g^{-1}) and a network like structure having an excellent capacitance of 292.64 F/g at current density 0.78 A/g. Further, this material possesses excellent cycling stability, as electrochemical storage capacity has maintained after 250 cycles. Importantly, this works gives a new source for the preparation of an electroactive carbon which is cheap, eco-friendly, sustainable, and high electroactive material with additional significance for environmental pollution and wastage management.

This chapter optimizes a bio-waste derived porous and electroactivecarbon which is ECC 800. Further enhancement in their electrochemical performance is always desired. In order to this, functionalization and modification have performed further and discussed in the next chapter.